

## ARTICLE

# DFT Study of Benzofuroxan Synthesis Mechanism from 2-Nitroaniline via Sodium Hypochlorite

Chun-yuan Hou<sup>a</sup>, Xiao-fang Chen<sup>a</sup>, Jian-yong Liu<sup>a\*</sup>, Wei-peng Lai<sup>b</sup>, Bo-zhou Wang<sup>b</sup><sup>a</sup>. State Key Laboratory of Molecular Reaction Dynamics, Dalian Institute of Chemical Physics, Chinese Academy of Sciences, Dalian 116023, China<sup>b</sup>. Xi'an Modern Chemistry Research Institute, Xi'an 710065, China

(Dated: Received on January 1, 2010; Accepted on March 31, 2010)

The oxidative cyclization reaction of 2-nitroaniline via sodium hypochlorite to yield benzofuroxan is investigated by the hybrid density functional theory B3LYP/6-31G(d,p) method. Solvent effects are estimated with the polarizable continuum model to optimize structures. The title reaction is predicted to undergo two pathways, each of which is a stepwise process. Path A includes four steps, namely oxidization, H-attack, hydrolysis, and cyclization. Path B involves the nucleophilic attack of OH<sup>-</sup> to the H atom of the N-H bond and the proton transfer to the N atom of amino group leading to the cleavage of the N-H single bond in the amino group. The calculated results indicate that path A is favored mechanism for the title reaction. Furthermore, it is rational for one water molecule serving as a bridge to assist in the hydrolysis step of Path A and our calculations exhibit that this process is the rate-determining step.

**Key words:** Benzofuroxan, Density functional theory, 2-Nitroaniline

## I. INTRODUCTION

Benzofuroxan-1-oxide (BFO) has received attention since 1960's for its widespread and long-term use in biochemical, pharmacological, and military field [1–5]. Conventionally, BFO is synthesized from the pyrolysis of ortho-substituted aryl azides (Fig.1(a)) [6], which is one of the oldest synthesis methods of BFO [6–9]. Great development has been made in recent years in the study on the synthesis of benzofuroxan, especially on the synthesis methods and techniques of oxidizing 2-nitroaniline with sodium hypochlorite (Fig.1(b)) [8, 9]. This method is more security, compared with the standard route of the pyrolysis of ortho-substituted aryl azides toward BFO.

The mechanism of the title reaction was first reported by Green *et al.* (Fig.1(c)) [10]. In their study, the first step is the nucleophilic attack of OH<sup>-</sup> to the H atom of the N-H bond and the proton transfer to the N atom of amino group leading to the cleavage of the N-H single bond in the amino group. The reaction continues with subsequent oxidization, loss of OH<sup>-</sup> and cyclization to the end. This mechanism was analyzed by Chapman *et al.*, in which the oxidization step and the factors affecting the course of the reaction have been investigated and a detailed reaction mechanism has been suggested

(Fig.1(d)) [11]. However, neither of the steps has been clearly described as rate determining.

It is well known that one of the most challenges of theoretical chemistry is to explore the correct mechanism. B3LYP method in density functional theory (DFT) is effective for theoretical studies of the ring chain tautomerism of BFO [12–18] and the mechanism of pyrolysis of 2-nitrophenyl azide for synthesizing BFO [6]. However, to our best knowledge, the mechanism of the formation of BFO from *o*-nitroaniline is unclear at the theoretical level up to now.

In this work, we model and clarify the reaction mechanism by using the DFT theory, we have not only investigated the reaction mechanism suggested by Green *et al.* [10], but also suggest a new mechanism including oxidization, H-attack, dehydration, and cyclization steps, which is thermally and kinetically in advantage.

## II. COMPUTATIONAL METHODS

All the calculations are performed with the Gaussian 03 program [19] on a Lenovo server. The hybrid B3LYP functional in conjunction with the 6-31G(d,p) basis sets are applied to the optimizations of all the stationary points. Harmonic vibrational frequencies are analyzed at the same level of optimization to characterize the nature of stationary points as true minima with no imaginary frequencies or transition states with only one imaginary frequency and to provide thermodynamic quantities such as thermal corrections to energy and Gibbs

\* Author to whom correspondence should be addressed. E-mail: beam@dicp.ac.cn, Tel.: +86-411-84379195

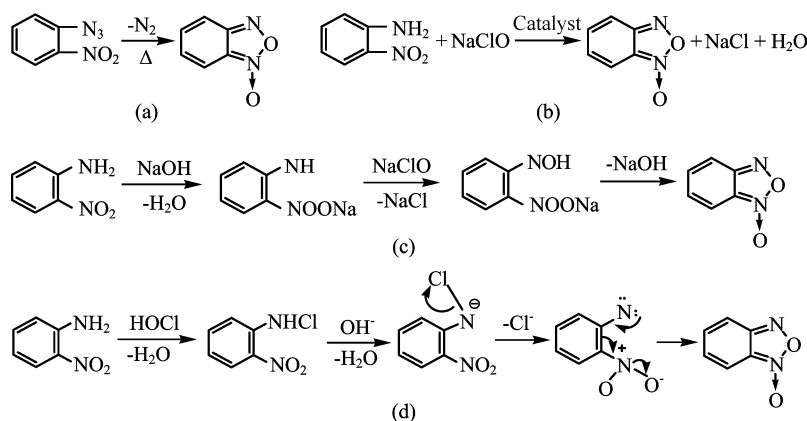


FIG. 1 Scheme of the reaction. (a) BFO is synthesized from the pyrolysis of ortho-substituted aryl azides. (b) The synthesis methods and techniques of oxidizing 2-nitroaniline with sodium hypochlorite. (c) The mechanism of the title reaction was first reported by Green *et al.* [10]. (d) Detailed reaction mechanism was suggested by Chapman and Dyall [11].

free energy. To simulate the title reaction in different solution, solvent effects are estimated with the polarizable continuum model (PCM) implemented in the Gaussian 03 to optimize structures; we have used the dielectric constants 24.55, 2.247, and 78.39 at 298.15 K for CH<sub>3</sub>CH<sub>2</sub>OH, H<sub>2</sub>O, and C<sub>6</sub>H<sub>6</sub>, respectively. In this continuum model,  $\Delta E_0$  are the zero-point energy (ZPE) corrected relative electronic energies in the above solvents. Free energies  $\Delta G$  are calculated with the standard statistical thermodynamics at 298.15 K. Corrections of the transition states between designated local minima are confirmed by intrinsic reaction coordinate (IRC) calculations at the same level. Nonadiabatic effects have been neglected, although they play some role in most chemical reactions [20].

### III. RESULTS AND DISCUSSION

For the title reaction, two pathways, path A (Fig.2(a)) and path B (Fig.2(b)), are explored in this work. Additionally, two channels may occur for the formation of PC3 in path A, channel 1 is that RE is directly oxidized by sodium hypochlorite before the H-attack of PC6 to form PC3, channel 2 is firstly the H-attack of RE to PC2, and then PC2 is oxidized to form PC3.

Figures 3 and 4 show the relative energy profile in the multistep reactions, together with the optimized geometries of all reactants, transition states, intermediates, and products at the B3LYP/6-31G(d,p) level. In this work, we focus mainly on the reaction mechanism of this reaction, for which the van der Waals complexes are of minor importance.

#### A. Path A

##### 1. Channel 1

The first step is oxidizing the reactant 2-nitroaniline (RE) via sodium hypochlorite, that is, the complex

RC2, to conform PC6. Figure 3(a) shows that the located transition state TS7 is directly associated with the coupling of the Cl–O bond cleavage and O atom transfer to N atom, leading to PC6 and Cl<sup>−</sup>. In the transition state TS7, O atom directly head toward the lone pair of N atom with the N–O and O–Cl distance of 1.77 and 2.23 Å, respectively. Therefore, it is possible for the charge on O atom to transfer to Cl atom and to break O–Cl bond. We determine that the tautomerization of the O atom transfer from Cl to N is a favored process and the energies required to cleave the Cl–O bond are only 67.3, 68.6, 62.7, and 64.8 kJ/mol in the gas phase, ethanol, water, and benzene solution, respectively. The calculated active and free energy difference between those in the gas phase and C<sub>6</sub>H<sub>6</sub> solution are only 2.5 and 1.7 kJ/mol, respectively, moreover, the optimized geometries vary little in the gas phase and benzene solution, so we use the optimized geometry in the gas phase to calculate the station point energy in the ethanol and water polar solutions because of the converge problem.

To form a favorable geometry to be hydrolyzed, the reaction continues with the H-attack of PC6 to conform PC3. The results are shown in Fig.2(b). PC6 tends to be in plane structure because of the conjugation effect and the calculated activation barrier for the formation of PC3 are 79.8, 81.1, and 70.2 kJ/mol in the CH<sub>3</sub>CH<sub>2</sub>OH, H<sub>2</sub>O, and C<sub>6</sub>H<sub>6</sub> solution, respectively. The product PC3 is more stable than PC6, which makes the formation of PC3 thermodynamically favorable.

The next step is dehydration of PC3 to conform PC4. From the PC3 geometry, TS4 should be a six-member cycle structure, from the geometric angle, we can see for the six-member cycle structure, there is much of ring constraint and because of the conjugation effect, no transition state can be found. Therefore, water-assisted mechanism is investigated for this step, one more water molecule is put as a bridge in this process to relax the ring constraint, thus, the transition state is re-

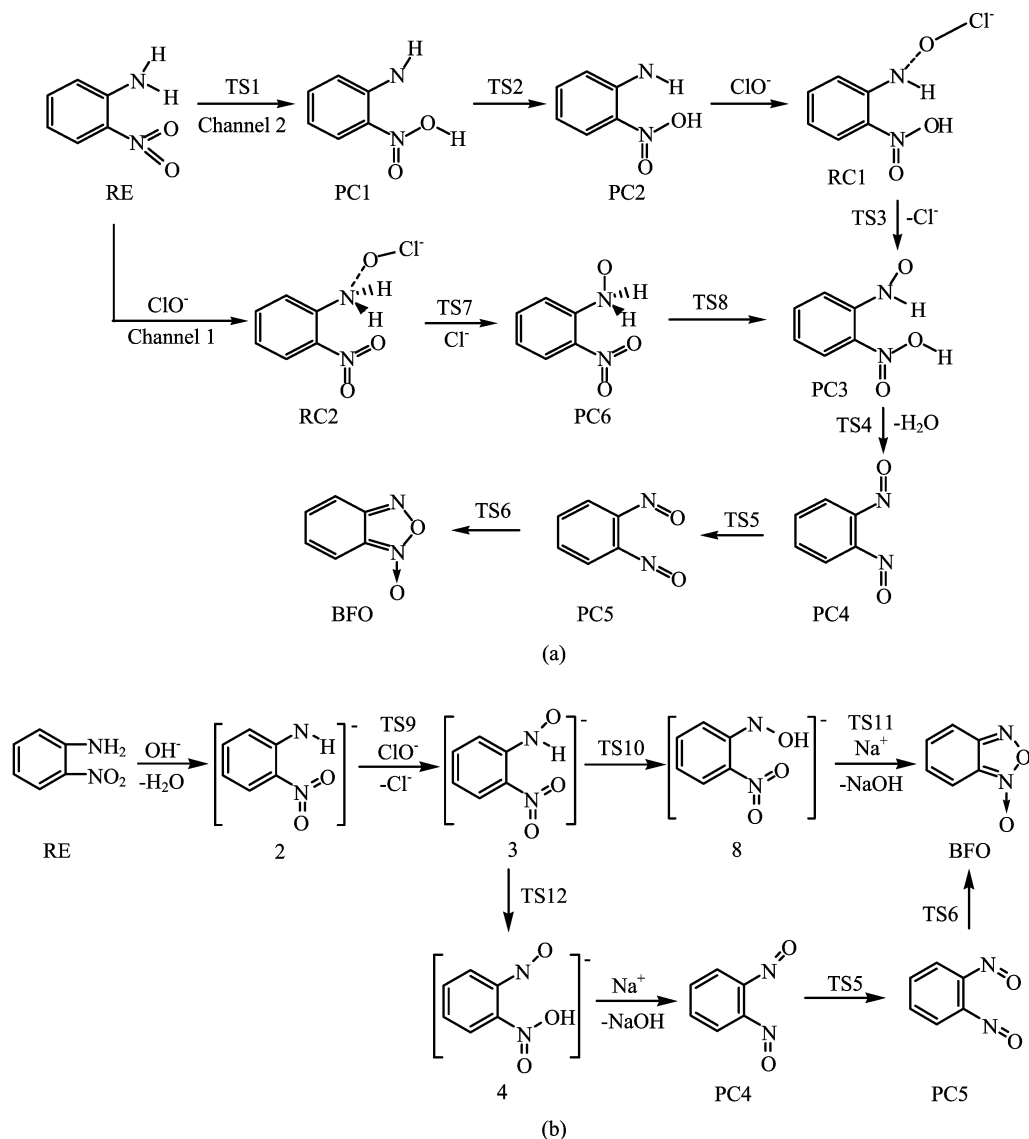


FIG. 2 For the title reaction, two pathways, path A (a) and path B (b), are explored in this work.

laxed and the angle strain is reduced. The results are shown in Fig.3(c). The calculated activation barrier for the formation of PC4 are 79.0, 79.8, and 63.9 kJ/mol in the  $\text{CH}_3\text{CH}_2\text{OH}$ ,  $\text{H}_2\text{O}$ , and  $\text{C}_6\text{H}_6$  solution, respectively. In experimentally, the reaction rate is faster in  $\text{CH}_3\text{CH}_2\text{OH}$  and  $\text{H}_2\text{O}$  than that in  $\text{C}_6\text{H}_6$  solution, this is the reason that  $\text{C}_6\text{H}_6$  is not dissolved in water, so the dehydration process in benzene is restricted. Our calculations exhibit that this process is the rate-determining step.

The reaction continues with the cyclization of PC4 tautomerize to PC6. Figure 2(d) shows all the activation barriers are lower than 28.0 kJ/mol, which suggest this step is very easy. As reported by Rauhut [14] in the ring chain tautomerism of BFO, our results are in agreement with theirs; therefore we don't study this step in detail.

## 2. Channel 2

As Pausacker and Scroggie suggested that H-attack as the first stage for the formation of benzofuroxan oxides from *o*-nitronanilines [7], we also investigate the first step of RE converts to PC1. The corresponding results are presented in Fig.3(e). Compared with channel 1, the free energy barriers increase to 155.9, 168.0, and 154.2 kJ/mol in the  $\text{CH}_3\text{CH}_2\text{OH}$ ,  $\text{H}_2\text{O}$ , and  $\text{C}_6\text{H}_6$  solution, respectively. The higher barrier for the H-attack is attributed to the reduction of the conjugation between phenyl group and the ONO group in TS1, moreover, that PC6 tend to be in plane structure also make the H-attack in channel 1 more favorable. Then PC2 is generated via the inversion of NH group in PC1. This step is exergonic ( $\Delta G$  about 135.0 kJ/mol), and the barrier height increases to about 250.8 kJ/mol, which is rela-

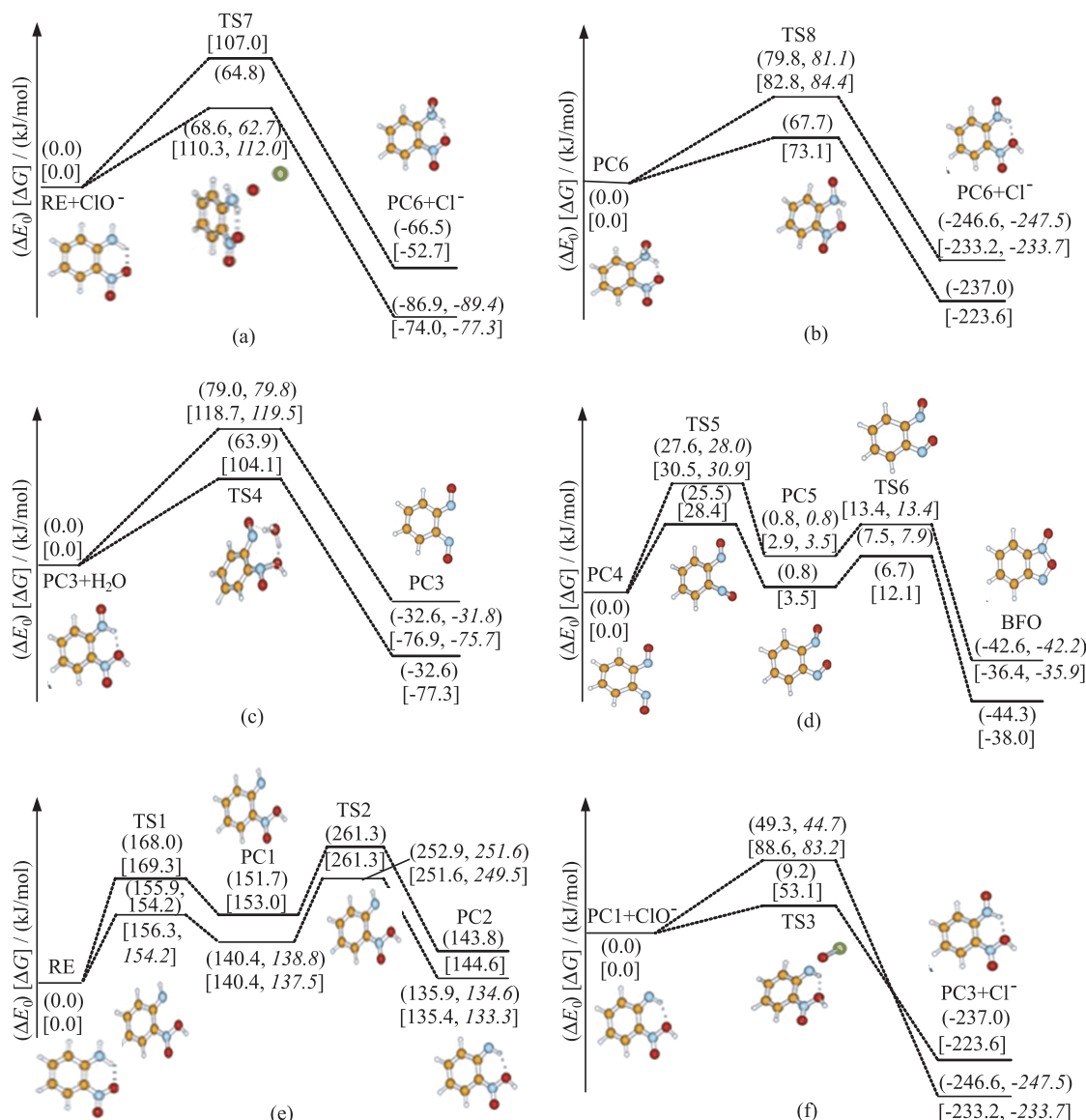


FIG. 3 Relative energy profile in path A. Under thick lined,  $(\Delta E_0)$  and  $[\Delta G]$  in the benzene solution; under thin lined,  $(\Delta E_0)$  and  $[\Delta G]$  with regular format are in the ethanol and those in italic format are in water solution. Hydrogen bonding are shown by dashed line. (a) In the first step in channel 1, (b) in the second step via H-attack mechanism in channel 1, (c) in the dehydration process via water-assisted mechanism in channel 1, (d) in the cyclization process of PC4 to BFO, (e) in the H-attack process in channel 2, (f) in the second step in channel 2.

tively high for the reaction, suggesting that this step is kinetically unfavorable at room temperature. Our results show channel 1 is more favorable than channel 2.

The second step is oxidizing PC2 via sodium hypochlorite to conform PC3 (Fig.2(f)). PC3 is almost planar due to the conjugation effect throughout the molecular. Compared with the first step in channel 1, in the transition state TS3, the dihedral angle,  $\angle \text{ClONC}$ , is bigger and nearly  $180^\circ$ , O atom directly head toward the lone pair of N atom with the N–O and O–Cl distance of 2.04 and 1.99 Å, respectively. The tautomerization of the O atom transfer from Cl to N is a favored process and the energy required to cleave the

Cl–O bond decrease to 49.3, 44.7, and 9.2 kJ/mol in the  $\text{CH}_3\text{CH}_2\text{OH}$ ,  $\text{H}_2\text{O}$ , and  $\text{C}_6\text{H}_6$  solution, respectively. The reaction continues with the processes of dehydration and cyclization to form BFO to the end, which is the same as shown in channel 1.

Comparing channel 1 and channel 2, we can see that the reaction starts with RE via sodium hypochlorite in channel 1, which enhances the conjugation effect, moreover, PC3 is more stable than PC6, so it is more favorable than RE firstly H-attack to PC1 and then is oxidized in channel 2. The results show that channel 1 is a favored mechanism for the title reaction.

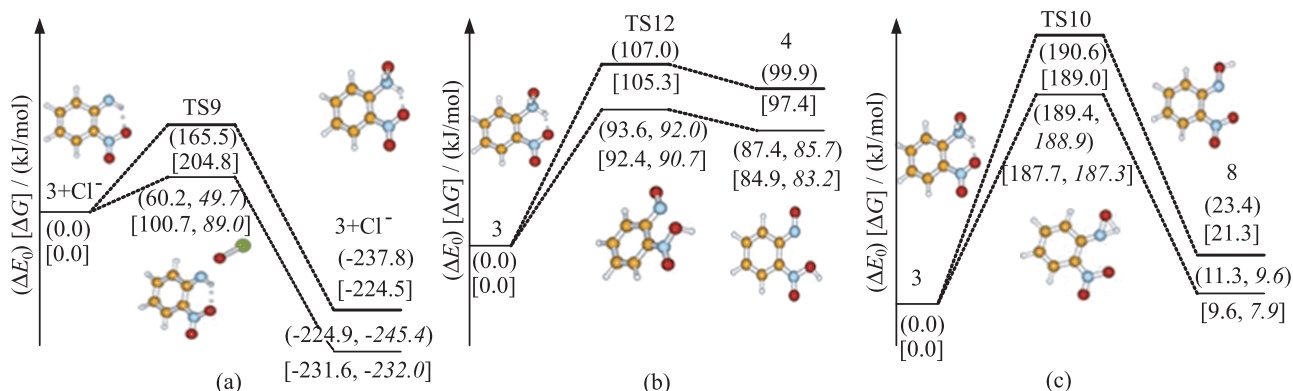


FIG. 4 Relative energy profile of path B. Under thick lined,  $(\Delta E_0)$  and  $[\Delta G]$  in the benzene solution; under thin lined,  $(\Delta E_0)$  and  $[\Delta G]$  with regular format are in the ethanol and those in italic format are in water solution. Hydrogen bonding are shown by dashed line. (a) In the second step, (b) in the O–H attack process, (c) in the O–H attack process.

## B. Path B

To be compared with path A, as reported by Green and Rowe [10], path B (Fig.2(b)) is also investigated in this work. The first step is RE converts to 2, however, as we know, the reaction of *o*-nitroaniline via NaOH is difficult and we can't find the transition states. Although the first step could not appear from this reaction, we also further study its subsequent processes.

The reaction continues with the oxidation, the second step is oxidizing molecule 2 via sodium hypochlorite, which is shown in Fig.4(a).

The effect of alkali metal hydrates is catalysis, the pathway continues with the O–H attack to loss the  $\text{OH}^-$  of molecule 4 or 8. There are two O–H attack channels. Figures 4 (b) and (c) show that the O–H attack in Path C is more favorable than the O–H attack in path B in both kinetics and thermodynamics.

The pathway continues with the loss of  $\text{OH}^-$ , because the environment tends to balance the charge, in the odd  $\text{Na}^+$  environment, the  $\text{OH}^-$  can be easily separated from molecule 4 or 8, this step is exergonic but no transition state can be found in this step. The reaction continues with the processes of cyclization to form BFO to the end, which is the same as shown in path A.

For the mechanism suggested by Chapman *et al.* [11], because the amount of HOCl in the solution is very small, the first process they suggested is difficult and no transition state can be found in our calculations, moreover, the loss of  $\text{Cl}^-$  in the last process is also very difficult. So we don't further study this mechanism in detail.

In path A, we can see the reaction barrier is higher in water and ethanol polar solution than that in benzene nonpolar solution, however, in benzene solution the dehydration process will be restricted and slow down the reaction. Our calculations are in agreement with previous experimental data.

## IV. CONCLUSION

DFT calculations at the B3LYP/6-31G(d,p) level is used to study the oxidative cyclization reactions mechanism between 2-nitroaniline and sodium hypochlorite to form benzofuroxan. A multistep reaction profile is found. IRC calculations provide the potential energy surface. Finally, the activation and free energies of all reactions are given. Path A includes four steps, namely oxidization, H-attack, dehydration, and cyclization. Path B involves the nucleophilic attack of  $\text{OH}^-$  to the H atom of the N–H bond and the proton transfer to the N atom of amino group leading to the cleavage of the N–H single bond in the amino group. The calculated results indicate that channel 1 in path A is favored mechanism for the title reaction. Furthermore, it is rational for one water molecule served as a bridge to assist in the dehydration step and our calculations exhibit that this process is the rate-determining step.

- [1] J. C. Halle, D. Vichard, M. J. Pouet, and F. Terrier, *J. Org. Chem.* **62**, 7178 (1997).
- [2] P. Sepulcri, J. C. Halle, R. Goumont, D. Riou, and F. Terrier, *J. Org. Chem.* **64**, 9254 (1999).
- [3] B. Heyne, C. Beddie, and J. C. Scaiano, *Org. Biomol. Chem.* **5**, 1454 (2007).
- [4] M. Onoda, H. Tokuyama, S. Uchiyama, K. Mawatari, T. Santa, K. Kaneko, K. Imai, and K. Nakagomi, *Chem. Commun.* 1848 (2005).
- [5] K. J. Hwang, I. Jo, Y. A. Shin, S. Yoo, and J. H. Lee, *Tetrahedron Lett.* **36**, 3337 (1995).
- [6] G. Rauhut and F. Eckert, *J. Phys. Chem. A* **103**, 9086 (1999).
- [7] K. H. Pausacker and J. G. Scroggie, *J. Chem. Soc.* 4499 (1954).
- [8] H. Faeh, Ciba Geigy Corp., U.S. Patent No.4185018, (1980).

- [9] F. B. Mallory, T. L. Cairns, and H. E. Simmons, *Org. Synth.* **4**, 74 (1963).
- [10] A. G. Green and F. M. Rowe, *J. Chem. Soc.* 2443 (1912).
- [11] K. J. Chapman and L. K. Dyllal, *Aust. J. Chem.* **37**, 341 (1984).
- [12] K. L. Han and G. Z. He, *J. Photochem. Photobiol. C: Photochem. Rev.* **8**, 56 (2007).
- [13] T. S. Chu and K. L. Han, *Phys. Chem. Chem. Phys.* **10**, 2431 (2008).
- [14] G. Rauhut, *J. Comput. Chem.* **17**, 1848 (1996).
- [15] G. J. Zhao and K. L. Han, *J. Phys. Chem. A* **111**, 2469 (2007).
- [16] Z. Skrinarova, K. Bowden, and W. M. F. Fabian, *Chem. Phys. Lett.* **316**, 531 (2000).
- [17] R. J. Li, K. L. Han, F. E. Li, R. C. Lu, G. Z. He, and N. Q. Lou, *Chem. Phys. Lett.* **220**, 281 (1994).
- [18] J. Stevens, M. Schweizer, and G. Rauhut, *J. Am. Chem. Soc.* **123**, 7326 (2001).
- [19] M. J. Frisch, G. W. Trucks, H. B. Schlegel, G. E. Scuseria, M. A. Robb, J. R. Cheeseman, G. Scalmani, V. Barone, B. Mennucci, G. A. Petersson, H. Nakatsuji, M. Caricato, X. Li, H. P. Hratchian, A. F. Izmaylov, J. Bloino, G. Zheng, J. L. Sonnenberg, M. Hada, M. Ehara, K. Toyota, R. Fukuda, J. Hasegawa, M. Ishida, T. Nakajima, Y. Honda, O. Kitao, H. Nakai, T. Vreven, J. A. Montgomery, Jr., J. E. Peralta, F. Ogliaro, M. Bearpark, J. J. Heyd, E. Brothers, K. N. Kudin, V. N. Staroverov, R. Kobayashi, J. Normand, K. Raghavachari, A. Rendell, J. C. Burant, S. S. Iyengar, J. Tomasi, M. Cossi, N. Rega, J. M. Millam, M. Klene, J. E. Knox, J. B. Cross, V. Bakken, C. Adamo, J. Jaramillo, R. Gomperts, R. E. Stratmann, O. Yazyev, A. J. Austin, R. Cammi, C. Pomelli, J. W. Ochterski, R. L. Martin, K. Morokuma, V. G. Zakrzewski, G. A. Voth, P. Salvador, J. J. Dannenberg, S. Dapprich, A. D. Daniels, O. Farkas, J. B. Foresman, J. V. Ortiz, J. Cioslowski, and D. J. Fox, *Gaussian 03 (Revision C.02)*, Wallingford, CT: Gaussian, Inc., (2004).
- [20] T. S. Chu, Y. Zhang, and K. L. Han, *Int. Rev. Phys. Chem.* **25**, 201 (2006).